Molecular Crystals and Liquid Crystals

ISSN: 1542-1406 (Print) 1563-5287 (Online) Journal homepage: http://www.tandfonline.com/loi/gmcl20

Nanostructures on the Basis of Porous Alumina with Intercalated with Cholesteric Liquid Crystal

Anatoliy Andrushchak, Zenon Hotra, Zinoviy Mykytyuk, Taras Prystay, Orest Sushynskyi & Maria Vistak

To cite this article: Anatoliy Andrushchak, Zenon Hotra, Zinoviy Mykytyuk, Taras Prystay, Orest Sushynskyi & Maria Vistak (2015) Nanostructures on the Basis of Porous Alumina with Intercalated with Cholesteric Liquid Crystal, Molecular Crystals and Liquid Crystals, 611:1, 132-138, DOI: 10.1080/15421406.2015.1030201

To link to this article: http://dx.doi.org/10.1080/15421406.2015.1030201

Published online: 06 Jul 2015.

Mol. Cryst. Liq. Cryst., Vol. 611: pp. 132–138, 2015

ISSN: 1542-1406 print/1563-5287 online
DOI: 10.1080/15421406.2015.1030201

Nanostructures on the Basis of Porous Alumina with Intercalated with Cholesteric Liquid Crystal

ANATOLIY ANDRUSHCHAK,[1] ZENON HOTRA,[1,2]
ZINOVIY MYKYTYUK,[1] TARAS PRYSTAY,[1]
OREST SUSHYNSKYI,[1,2,*] AND MARIA VISTAK[3]

[1]Rzeszow University of Technology, Rzeszow, Poland
[2]Lviv Polytechnic National University, Lviv, Ukraine
[3]Danylo Halytsky Lviv National Medical University, Lviv, Ukraine

The introduction of liquid crystal materials into the porous material host will help us to get optically active nanocomposites. Nanocomposite based on aluminum oxide host with cholesteric liquid crystal is characterized by a shift of bandwidth wavelength minimum. In case of intercalation of cholesteric liquid crystals into the pores of aluminum oxide host the shift of transmittance minimum into the short wave region are observed. We analyzed the ways, which indicate the deformation of the pitch of the cholesteric helix and showed the role of capillary forces in the deformation of the pitch of cholesteric liquid crystal.

Keywords porous material; cholesteric liquid crystal; deformation pitch; spectral characteristics

Introduction

Small scale systems are widely used as an element base of modern electronics. Some useful examples of such systems are silicon oxide, alumina, gallium phosphide etc. The important characteristics of porous materials are porosity, size and shape of pore, the distance between them, the spatial arrangement and morphology. These characteristics determine the physical properties of porous materials and will significantly affect by the nanostructures properties. The anisotropy of refractive index is an important parameter for the creation of optical sensors and photonic crystals. Porous alumina takes an important place and above all is characterized by the simplicity of manufacturing. The selection of the mode of etching provides the ability to control the size of pores and the distance between them which makes alumina unique in terms of its application as a solid state matrix. Usually such matrices are characterized by an ordered pore system with a surface density of 10^9-10^{10} cm^{-2}, and as result they have a high adsorption capacity. Technique for obtaining of a porous alumina allows changing the size of the pores and the distance between them in the range from tens to hundreds of nanometers [1]. Such flexibility opens up a wide field of application of porous alumina as a matrix for the creation of nanostructures.

Nanostructures based on porous matrices with ferromagnetic, ferroelectric piezoelectric, and optically active materials intercalated into pores is a promising material from point

*Address correspondence to Orest Sushynskyi, Lviv Polytechnic National University, S. Bandery str. 12, Lviv, Ukraine, 79013. Email: orestsy@yahoo.com

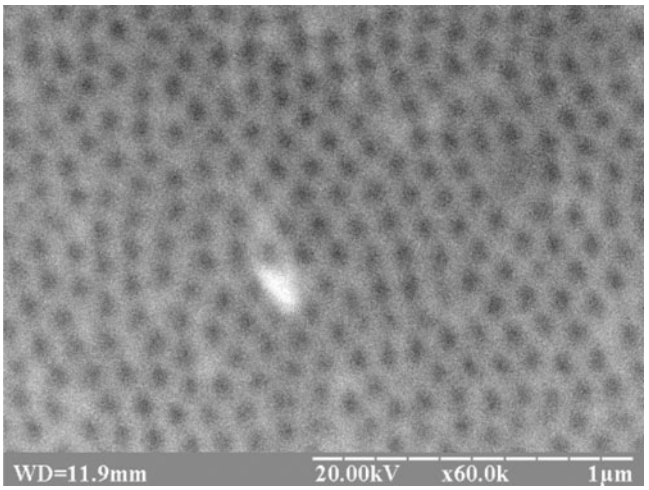

Figure 1. Scanning electron microscope image of alumina surface.

of view of further development of nanotechnologies [2, 3, 4, 5]. Matrices on the basis of alumina are easy to manufacture comparing with a large number of other mesoporous matrices [1].

Experimental

We used mesoporous alumina films of thickness of 96, 102, 115 microns and a pore size of 20, 35, 50 nm, respectively. Study of the surface morphology of films was carried out with the scanning electron microscope (SEM). These micrographs (Fig. 1.) show hexagonal structure of the films. Pores in the form of cylindrical channels oriented normally to the film surface.

Absolute values of translation vectors of a triangular lattice of pores are equal to each other, which is an evidence of a hexagonal. Since the films are highly adsorptive their properties significantly change over time due to absorbance of moisture form air. Therefore, before filling the porous matrix should be kept in a vacuum of 10^{-4}–10^{-5} Pa [6, 7]. X-ray study of Al_2O_3 films showed they have an amorphous structure. Experimental study of transmission spectra of nanostructures and their components are carried out by means of the Ocean Optics© USB2000+ spectrometer in the range of 200–1200 nm at room temperature. The porosity of the alumina samples was determined through the analysis of transmittance spectra of films measured at different angles of incidence.

For the determination of anisotropy of refractive index we use the transmittance spectra of samples, which are placed between crossed polarizers in range of 200–1200 nm at different angles of incidence light. The interference maximum and minimum are in the transmittance spectra figures. Analysis of transmission spectra between crossed polarizers, normalized to its transmission spectra between parallel polarizers at different angles of incidence of optical radiation are as follows:

$$\Delta n_{max} = \frac{\lambda}{2d_{ef}} = \frac{\lambda \cos\theta}{2d} \tag{1}$$

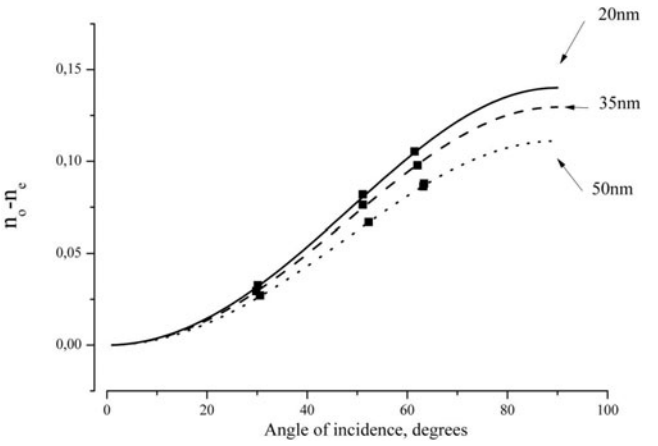

Figure 2. The anisotropy of the refractive index of Al_2O_3 of 20, 35 and 50 nm as a function of the angle of incidence.

$$\Delta n_{min} = \frac{\lambda}{d_{ef}} = \frac{\lambda \cos\theta}{d} \tag{2}$$

where λ – wavelength, corresponding to maximum or minimum of the interference pattern, θ – angle of refraction of the beam, d – sample thickness, d_{ef} – optical path length in the sample,

$$\theta = \arcsin\left(\frac{\sin\beta}{n}\right) \tag{3}$$

We plot $\Delta n = f(\beta)$, β – angle of incidence.

The analysis of transmittance spectra is shown, in case of normal light incident the interference image is not observed, but, in case of changing of incident angle the interference maximum and minimum are observed. From positions of spectral maximum and minimum at different angle of incidence, for samples with different diameter of pores, the dependencies of the anisotropy of the refractive index versus the angle of incidence (Fig. 2) were calculated.

For a uniaxial crystal angular dependence of the anisotropy of the refractive index is given by:

$$\Delta n\,(\theta) = n_0 \left(\frac{1}{\sqrt{\cos^2 + \left(\frac{n_0}{n_e}\right)^2 \sin^2\theta}} - 1 \right) \tag{4}$$

Using this expression it is possible to approximate the dependence of $\Delta n = f(\beta)$, and obtain values of n_0 and n_e. The results of calculation of the refractive index are shown on Table 1.

Obtained experimental dependencies were analyzed using model by Saito and Miyagi [8, 9, 10]. In this model, for $a \ll b \ll \lambda$, where a – radius of the pore, b – distance between pore

Table 1. The results of calculation of the refractive index for Al_2O_3

Material	Diameter of pores		
	20 nm	*35 nm*	*50 nm*
Al_2O_3			
Δn	0.14	0.13	0.11
n_0	1.56	1.53	1.54
n_e	1.70	1.66	1.65

cylinders, λ – wavelength. The analytical expression for the principal refractive indices of ordinary and extraordinary waves according to this model is:

$$n_0 = n_1 - \frac{\pi a^2}{2b^2} \cdot \frac{n_1^2 - n_2^2}{n_1} \tag{5}$$

$$n_e = n_1 - \frac{\pi a^2}{b^2} \cdot \frac{\left(n_1^2 - n_2^2\right) \cdot n_1}{n_1^2 + n_2^2} \tag{6}$$

where $n_1 = 1.76$; $n_2 = 1$; refractive indices of alumina in the visible range and of air which fills the pores.

Taking in to account our calculations for samples with diameters of pores 20, 35, 50 nm the porosity P are equal 22, 25, 24%.

Results and Discussion

Pores of the alumina were filled with cholesteric liquid crystal EE1 which has transition from the chiral nematic to the isotropic phase at 301 K. Filling of the mesoporous Al_2O_3 matrix with liquid crystal was carried out by direct intercalation of LC into the pores. Al_2O_3 sample was immersed in the LC and was kept in it at room temperaturefor 24 hours. No procedures to remove the residual layer of LC from the surface of the alumina were carried out.

Mesoporous matrix is transparent throughout the visible range of spectrum. The spectrum of the cholesteric LC shows a well distinctive minimum at a wavelength of 560 nm caused by a selective reflection due to the formation of a special periodic cholesteric helical structure.

Figure. 3. shows typical transmission spectrum of nanostructures with two minima. First minimum correspondsis caused by the transmittance through the LC on the surface, and the second minimum–LC located in the pores.

On the Figs. 4 and 5. are shown the transmittance minimum of nanostructures with LC in the pores of the film as a function of diameter of pores.

As we can see from the dependence (Fig. 4) an increase in the diameter of pores in alumina leads to an increase in pitch of the cholesteric helix of intercalated LC, and pitch is trying to reach its equilibrium state. And as we can see from dependence (Fig. 5) of transparence minimum versus diameters of pores for liquid crystal placed on film surface, the decreasing in the pitch of the cholesteric helix is occurred. Increasing the diameters of pores leads to a decrease in the pitch of cholesteric helix. Obtained dependencies show

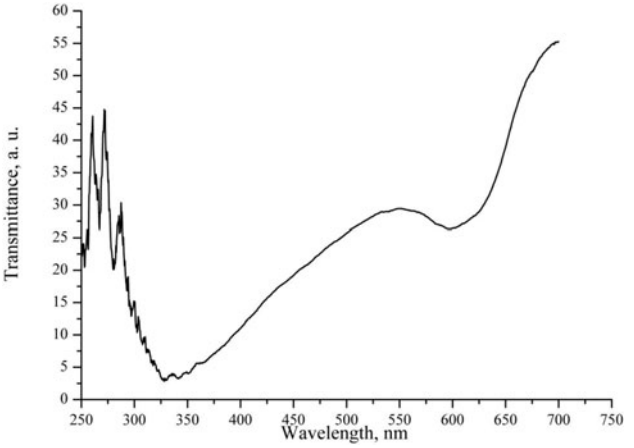

Figure 3. Spectrum of the selective reflection of light from alumina film with a LC.

that the deformation of the pitch of cholesteric helix strongly depends on the size of the confining surface (pores).

Let us analyze the nature of the forces acting on the helical pitch in restricted geometry. On a porous film with liquid crystalline material act both a surface and capillary forces. As it was described in few papers [7, 13] the implementation into porous matrix the ferroelectrics liquid crystals the displacement of the phase transition temperature are observed. The one of the reason of this displacement is explained by the different between coefficients of the thermal expansion of the ferroelectrics liquid crystal and the porous matrix. The thermoelastic stress caused by differences between these coefficients, leads to changes of the physical properties such materials in pores. [7]. The change of the pitch of cholesteric helix in the pores of the matrix can be caused by thermoelastic stresses arising from the different thermal expansion coefficients of alumina and cholesteric liquid crystal. The shift

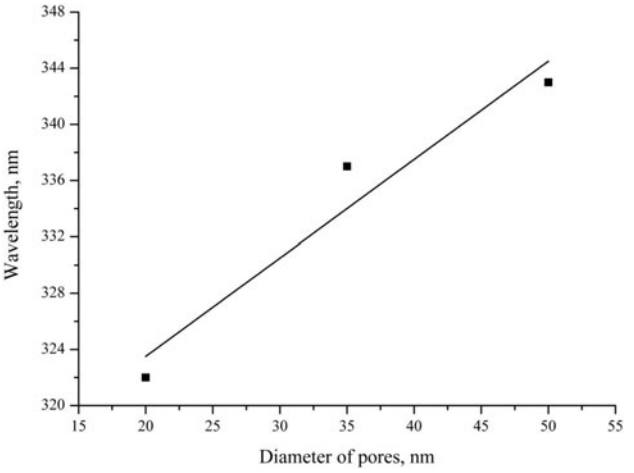

Figure 4. The transmittance minimum of nanostructures with LC in the pores of the film as a function of diameter of pores.

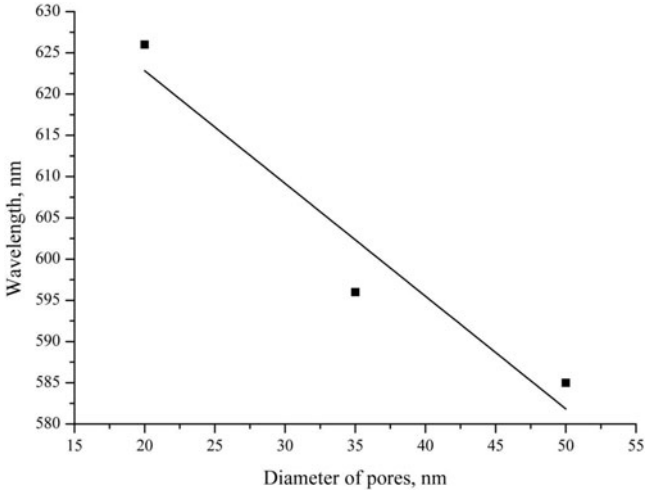

Figure 5. The transmittance minimum of nanostructures with LC on the surface of the film as a function of diameter of pores.

of the phase transition temperature is the result of changes of the order parameter and therefore of the pitch of the cholesteric helix.

Conclusion

In summary we have investigated the transmittance spectra of nanocomposite based on aluminum oxide host with cholesteric liquid crystal. Such nanocomposite are characterized with two minima. The surface and capillary forces are influent on a porous film with liquid crystalline material. We confirmed that the increasing of diameters of pores leads to decreasing the pitch of cholesteric helix. Obtained dependencies show that the deformation of the pitch of cholesteric helix strongly depends on the size of the confining surface (pores). The change of the pitch of cholesteric helix in the pores of the matrix can be caused by thermoelastic stresses.

References

[1] Yasui, K., Nishio, K., Nunokawa, H., & Masuda, H. (2005). *J. Vac. Sci. Tech. B.*, *23*, 4, L9.
[2] Masuda, H., Yada, K., & Osaka, A. (1998). *Jpn. J. Appl. Phys.*, *37*, L1340.
[3] Jessensky, O., Muller, F., & Gosele, U. (1998). *Applied Physics Letters.*, *72*, 10, 1173.
[4] De Laet, J., Terryn, H., & Vereecken, J. (1998). *Thin Solid Films.*, *320*, 2, 241.
[5] Nielsch, K., Choi, J., Schwirn, K., Wehrspohn Ralf, B., & Gösele, U. (2002). *Nano Lett.*, *2*, 7, 677.
[6] Golitsyna, O. M., Drozhdin, S. N., Nechaev, V. N., Viskovatykh, A. V., Kashkarov, V. M., Gridnev, A. E., & Chernyshev, V. V. (2013). *FTT*, *55*, 3, 479.
[7] Golitsyna, O. M., Drozhdin, S. N., Gridnev, A. E., Chernyshev, V. V., & Zenin, I. E. (2010). *Izv. RAN. Ser. Fiz.*, *74*, 9, 1347.
[8] Saito, M., & Miyagi, M. (1989). *Appl. Opt.*, *28*, 15, 3529.
[9] Saito, M. & Miyagi, M. (1989). *Opt. Soc. Am. A*, *6*, 12, 1895.
[10] De Laet, J., Terryn, H., & Vereecken, J. (1998). *320*, 241.
[11] Golitsyna, O. M., Drozhdin, S. N., & Gridnev, A. E. (2012). *FTT*, *54*, 10, 1839.

[12] Mel'nikov, V. A., Golovan', L. A., Timoshenko V., Yu., Kashkarov, P. K., Gavrilov, S. A., Kravchenko, D. A., Parkhomenko, Yu. N., & Skryleva, E. A. (2003). Vestnik Mosk. Un-ta. Seriya 3. Fizika. *Astronomiya*, *4*, 43.
[13] Baryshnikov, S. V., Charnaya, E. V., Stukova, E. V., Milinskii, A. Yu., & Cheng, T. (2010). *FTT*, *52*, 7, 1347.